Conflict of interest statement

None declared.

References

1. Boring CC, Squires TS, Tong T, Montgomery S. Cancer statistics, 1994. *CA Cancer J Clin* 1994;44:7–26.
2. Ministry of Health LaW. Statistics of Japan 2004;290.
3. Otsuji E, Yamaguchi T, Sawai K, et al. Recent advances in surgical treatment have improved the survival of patients with gastric carcinoma. *Cancer* 1998;82:1233–7.
4. Sakamoto Y, Ohyama S, Yamamoto J, et al. Surgical resection of liver metastases of gastric cancer: an analysis of a 17-year experience with 22 patients. *Surgery* 2003;133:507–11.
5. Hwang SE, Yang DH, Kim CY. Prognostic factors for survival in patients with hepatic recurrence after curative resection of gastric cancer. *World J Surg* 2009;33:1468–72.
6. Yagi Y, Seshimo A, Kameoka S. Prognostic factors in stage IV gastric cancer: univariate and multivariate analyses. *Gastric Cancer* 2000;3:71–80.
7. Watanabe R, Johzaki H, Iwasaki H, et al. A new tumor-associated antigen defined by a monoclonal antibody directed to gastric adenocarcinoma. *Cancer* 1993;71:2439–47.
8. Arakawa F, Yamamoto T, Kanda H, et al. cDNA sequence analysis of monoclonal antibody FU-MK-1 specific for a transmembrane carcinoma-associated antigen, and construction of a mouse/human chimeric antibody. *Hybridoma* 1999;18:131–8.
9. Yamamoto T, Arakawa F, Nakamura K, et al. Enhanced antitumor activity of a combination treatment with a mouse/human chimeric anti-MK-1 antibody and lymphokine-activated killer cells in vitro and in a severe combined immunodeficient mouse xenograft model. *Cancer Immunol Immunother* 1999;48:165–71.
10. Du W, Ji H, Cao S, et al. EpCAM: a potential antimetastatic target for gastric cancer. *Dig Dis Sci* 2010;55:2165–71.
11. Schmidt M, Scheulen ME, Dittrich C, et al. An open-label, randomized phase II study of adecatumumab, a fully human anti-EpCAM antibody, as monotherapy in patients with metastatic breast cancer. *Ann Oncol* 2010;21:275–82.
12. Association JGC. Japanese Classification of Gastric Carcinoma. Tokyo: Kanehara & Co 1999.
13. Lauren P. The two histological main types of gastric carcinoma: diffuse and so-called intestinal-type carcinoma. An attempt at a histo-clinical classification. *Acta Pathol Microbiol Scand* 1965;64:31–49.
14. Scheele J, Stangl R, Altendorf-Hofmann A. Hepatic metastases from colorectal carcinoma: impact of surgical resection on the natural history. *Br J Surg* 1990;77:1241–6.
15. Scheele J, Stang R, Altendorf-Hofmann A, Paul M. Resection of colorectal liver metastases. *World J Surg* 1995;19:59–71.
16. Minagawa M, Makuuchi M, Torzilli G, et al. Extension of the frontiers of surgical indications in the treatment of liver metastases from colorectal cancer: long-term results. *Ann Surg* 2000;231:487–99.
17. Ochiai T, Sasako M, Mizuno S, et al. Hepatic resection for metastatic tumours from gastric cancer: analysis of prognostic factors. *Br J Surg* 1994;81:1175–8.
18. Miyazaki M, Itoh H, Nakagawa K, et al. Hepatic resection of liver metastases from gastric carcinoma. *Am J Gastroenterol* 1997;92:490–3.
19. Maehara Y, Moriguchi S, Kakeji Y, et al. Pertinent risk factors and gastric carcinoma with synchronous peritoneal dissemination or liver metastasis. *Surgery* 1991;110:820–3.
20. Okuyama K, Isono K, Juan IK, et al. Evaluation of treatment for gastric cancer with liver metastasis. *Cancer* 1985;55:2498–505.
21. Bines SD, England G, Deziel DJ, et al. Synchronous, metachronous, and multiple hepatic resections of liver tumors originating from primary gastric tumors. *Surgery* 1993;114:799–805; discussion 804–795.
22. Yamashita H, Kitayama J, Ishikawa M, Nagawa H. Tissue factor expression is a clinical indicator of lymphatic metastasis and poor prognosis in gastric cancer with intestinal phenotype. *J Surg Oncol* 2007;95:324–31.
23. Takahashi Y, Cleary KR, Mai M, et al. Significance of vessel count and vascular endothelial growth factor and its receptor (KDR) in intestinal-type gastric cancer. *Clin Cancer Res* 1996;2:1679–84.
24. Hamada Y, Nakayama Y, Mizoguchi M, et al. MK-1 expression in carcinoma of the ampulla of Vater as a predictor of improved prognosis after surgical resection. *Cancer Lett* 2006;243:211–6.
25. Ikeda T, Nakayama Y, Hamada Y, et al. FU-MK-1 expression in human gallbladder carcinoma: an antigenic prediction marker for a better postsurgical prognosis. *Am J Clin Pathol* 2009;132:111–7.
26. Munz M, Baeuerle PA, Gires O. The emerging role of EpCAM in cancer and stem cell signaling. *Cancer Res* 2009;69:5627–9.
27. Trzpis M, McLaughlin PM, de Leij LM, Harmsen MC. Epithelial cell adhesion molecule: more than a carcinoma marker and adhesion molecule. *Am J Pathol* 2007;171:386–95.
28. Yasuda K, Adachi Y, Shiraishi N, et al. Prognostic effect of lymph node micrometastasis in patients with histologically node-negative gastric cancer. *Ann Surg Oncol* 2002;9:771–4.
29. Songun I, Litvinov SV, van de Velde CJ, et al. Loss of Ep-CAM (CO17–1A) expression predicts survival in patients with gastric cancer. *Br J Cancer* 2005;92:1767–72.
30. Went P, Vasei M, Bubendorf L, et al. Frequent high-level expression of the immunotherapeutic target Ep-CAM in colon, stomach, prostate and lung cancers. *Br J Cancer* 2006;94:128–35.
31. Wenqi D, Li W, Shanshan C, et al. EpCAM is overexpressed in gastric cancer and its downregulation suppresses proliferation of gastric cancer. *J Cancer Res Clin Oncol* 2009;135:1277–85.

Gastric Cancer (2013) 16:537–542
DOI 10.1007/s10120-012-0228-4

ORIGINAL ARTICLE

Characteristics of intramural metastasis in gastric cancer

Tatsuya Hashimoto · Kuniyoshi Arai · Yuichi Yamashita · Yoshiaki Iwasaki · Tsunekazu Hishima

Received: 16 May 2012 / Accepted: 17 December 2012 / Published online: 13 January 2013

Abstract

Background Intramural metastasis (IM) in gastric cancer is rare. However, it often occurs with esophageal squamous cell carcinoma and has been reported to have a poor prognosis.

Methods In 4,714 cases of gastric cancer that underwent gastrectomy, the clinicopathological features and postoperative prognoses of 29 cases with IM were evaluated and compared with 2,770 cases of advanced gastric cancer without IM.

Results Of the 4,714 cases, 29 (0.6 %) were histopathologically diagnosed with gastric cancer with IM. There were significant differences in the number of lymph node metastases, capillary invasion, and stage grouping between cases with IM and advanced gastric cancer without IM. Metastasis size was approximately within 2 cm, and many metastases occurred within 2 cm of the primary lesion. Multiple metastases were observed in 38 % of cases and occurred mainly in the submucosa and muscularis propria. IM was detected preoperatively in 17.2 % of cases and was present equally on both sides of the primary lesion. Nine cases had IM outside the stomach. The median survival time with IM was significantly less than in cases of advanced gastric cancer without IM ($p < 0.0001$). A subgroup of cases with IM within 1 cm of the primary lesion had a relatively favorable prognosis.

Conclusions The presence of IM is thought to be one of the most important prognostic factors in gastric cancer. Aggressive resection is recommended to increase long-term survival if curative resection is possible.

Keywords Stomach neoplasms · Gastric cancer · Lymphatic metastasis · Intramural metastasis · Prognosis

T. Hashimoto (✉) · Y. Yamashita
Department of Gastroenterological Surgery, Fukuoka University School of Medicine, 7-45-1 Nanakuma, Jonan-ku, Fukuoka 814-0180, Japan
e-mail: adams7230@me.com

K. Arai
Tokyo Metropolitan Health and Medical Treatment Corporation Toshima Hospital, 33-1 Sakae-cho, Itabashi-ku, Tokyo 173-0015, Japan

Y. Iwasaki
Department of Surgery, Tokyo Metropolitan Cancer and Infectious Diseases Center, Komagome Hospital, 3-18-22 Honkomagome, Bunkyo-ku, Tokyo 113-8677, Japan

T. Hishima
Department of Pathology, Tokyo Metropolitan Cancer and Infectious Diseases Center, Komagome Hospital, 3-18-22 Honkomagome, Bunkyo-ku, Tokyo 113-8677, Japan

Introduction

Intramural metastasis (IM) in gastric cancer has been rarely reported. However, esophageal squamous cell carcinoma is often accompanied by IM, and such cases have been reported to have a poor prognosis. As a result, the presence of IM with carcinoma is considered to be one of the most important prognostic factors [1–3]. There have been no detailed clinicopathological descriptions of IM in gastric cancer, to date. Therefore, we retrospectively conducted a clinicopathological study on the incidence of IM and its relationship to prognosis and survival.

Patients and methods

We reviewed 29 cases with IM in gastric cancer among 4,714 cases (0.6 %) who underwent gastrectomy between 1975 and 2004 at the Tokyo Metropolitan Cancer and Infectious Diseases Center (CICK), Komagome Hospital. Clinicopathological characteristics including age, gender, operation data, histological diagnosis, stage, and survival data were obtained from our hospital database and clinical records. Preoperative diagnosis was based on upper gastrointestinal barium studies, endoscopic examination, and computed tomography. Resected specimens were examined using standard hematoxylin and eosin staining. The gastric cancers were evaluated according to the "Japanese Classification of Gastric Carcinoma" (Japanese Gastric Cancer Association, 3rd English edition) [4].

Diagnostic criteria of IM

To diagnose IM histologically, we modified the criteria of Nishimaki et al. [1] as follows: (1) clearly separated from the primary tumor; (2) located in the wall of the esophagus, stomach, or duodenum; (3) having a gross appearance of a submucosal tumor without intraepithelial cancer extension; (4) having the same histological type as the primary tumor; and (5) lacking any evidence of intravascular growth.

These criteria discriminated IMs from multiple primary tumors in the esophagus or stomach and from intravascular tumor emboli around the primary tumor. A typical example of IM is shown in Fig. 1.

Statistical analysis

The association between factors was evaluated using the χ^2 test and Fisher's exact probability test. The significance of difference among means was determined using the Mann–Whitney *U* test. Survival rates were determined using the Kaplan–Meier method, and differences between survival curves were examined with the log-rank test. Statistical analyses were performed using the SAS software package Stat View, version 5.0 (SAS Institute, Cary, NC, USA). A result was considered statistically significant when the p value was <0.05.

Results

From 1975 to 2004, 4,714 patients with gastric cancers underwent gastrectomy at the CICK. Surgeries were as follows: 1,691 cases of total gastrectomy; 2,721 cases of

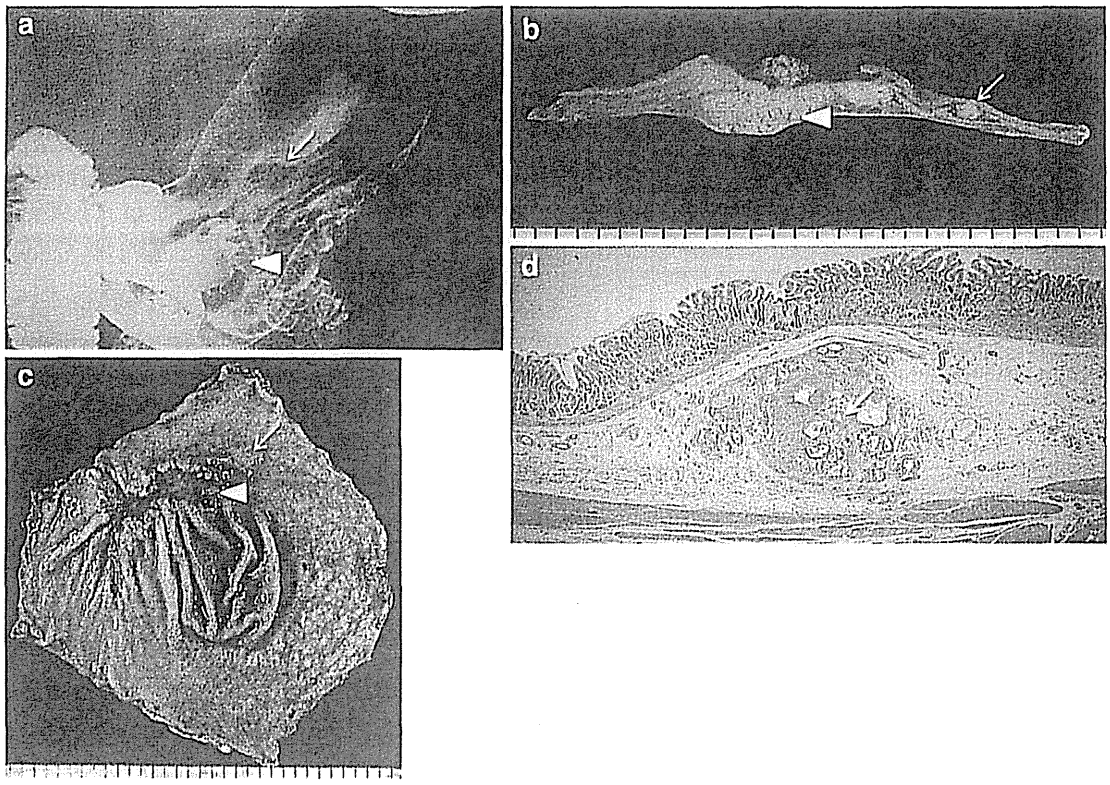

Fig. 1 A case of gastric cancer with intramural metastasis (IM). X-ray examination (a) and gross appearance of the resected specimen (b, c) show the primary tumor (*arrowheads*) and IM (*arrows*). The IM is clearly separated from the primary tumor and has the gross appearance of a submucosal tumor. d Histologically, IM (*arrow*) is present in the submucosal layer. Hematoxylin and eosin (H&E)

distal gastrectomy; 162 cases of proximal gastrectomy; 94 cases of segmentectomy; 11 cases of pancreaticoduodenectomy; 32 cases of pylorus-preserving gastrectomy; and 3 cases of segmental resection of the stomach. There were 1,915 cases of early cancer and 2,799 cases of advanced cancer. All 29 cases of IM were seen in advanced cancers, providing an onset frequency of 0.6 % of all resection cases and 1 % of advanced cancer cases. In IM cases, surgeries were as follows: 17 cases of total gastrectomy, 11 cases of distal gastrectomy, and 1 case of proximal gastrectomy.

The clinicopathological characteristics of gastric cancer with IM

To evaluate the clinicopathological characteristics of gastric cancer with IM, 29 cases of gastric cancer with IM were compared with 2,770 cases of advanced gastric cancer without IM (Table 1). The mean age of IM cases is higher than cases of advanced gastric cancer without IM. Histologically, IM cases occurred significantly more frequently in number of lymph node metastases, lymphatic invasion, vessel invasion, and advanced stage groupings compared with cases of advanced gastric cancer without IM. All IM cases showed marked lymph node metastasis and capillary invasion. There were no significant differences between these two groups with respect to gender, the main location of the primary tumor, tumor size, macroscopic type, histological type, depth of invasion, and residual tumor.

Characteristics of IM

The characteristics of IM are shown in Table 2. The mean IM size was 1.09 ± 1.10 cm (range, 0.2–6.0 cm). The number of IMs was one in 18 cases (62 %), two in 4 cases, three in 4 cases, four in 1 case, and five or more in 2 cases (multiple, 38 %). The layers affected by IM were 13 cases

Table 1 Patient characteristics of gastric cancer cases

	With IM ($n = 29$)		Advanced gastric cancer without IM		p value
	N	Percent (%)	*N*	Percent (%)	
Gender (male/female)	20/9	68/32	1,816/954	66/34	0.70
Age					
Mean ± SD (range)	66.4 ± 9.12 (48–81)	–	60.7 ± 12.26 (24–92)		0.04
Main location of primary tumor					
Upper/middle/lower	10/10/9	34/34/32	791/1,018/961	29/37/34	0.78
Tumor size (cm)	8.22 ± 4.02 (2.3–18.0)	–	8.12 ± 4.19 (1.2–25.0)		0.89
Macroscopic type					
1/2/3/4/5	2/5/15/4/3	7/17/52/14/10	97/760/988/433/492	4/27/35/16/18	0.82
Histological type					
Pap/tub1/tub2/por/sig/muc	4/3/9/9/2/2	14/10/31/31/7/7	321/429/507/988/366/159	12/15/18/36/13/6	0.51
Depth of invasion					
m/sm/mp/ss/se/si	0/0/2/5/15/7	0/0/7/17/52/24	0/0/285/1,031/1,076/378	0/0/10/37/39/14	0.07
Number of lymph node metastases					
0/1–2/3–6/7≤	0/2/8/19	0/7/28/65	604/541/592/1,033	22/20/21/37	0.0016
Distant metastasis site (liver/peritoneal/CY1)[a]	11 (5/8/1)	–	(168/477/–)	–	NA
Capillary invasion					
ly0/ly1/ly2/ly3	0/2/7/20	0/7/24/69	73/1,137/870/690	3/41/31/25	<0.0001
v0/v1/v2/v3	0/4/17/8	0/14/59/27	273/1,338/840/317	10/48/30/22	<0.0001
Residual tumor					
R0/R1, R2	14/15	48/52	1,753/1,017	63/37	0.12
Stage					
I B/II A/II B/III A/III B/IIIC/IV	0/1/2/3/3/11/11	0/4/0/10/10/38/38	184/331/352/346/358/283/916	7/12/13/12/13/10/33	0.0001

IM intramural metastasis, *pap* papillary adenocarcinoma, *tub 1* well-differentiated tubular adenocarcinoma, *tub 2* moderately differentiated tubular adenocarcinoma, *por* poorly differentiated adenocarcinoma, *sig* signet-ring cell carcinoma, *muc* mucinous cell carcinoma, *m* mucosa, *sm* submucosa, *mp* muscularis propria, *ss* subserosa, *se* serosa exposed, *se* adjacent structures, *NA* not assessable

[a] With overlapping

(45 %) in the submucosa (sm), 10 cases (34 %) in the muscularis propria (mp), 5 cases (17 %) in the subserosa (ss), and 1 (4 %) case in the serosa exposed (se). IM was detected preoperatively in 5 cases (17.2 %) using upper gastrointestinal barium studies and endoscopic examination. The mean distance between the IM and the primary tumor was 1.21 ± 0.94 cm (range, 0.1–5.5 cm). Eleven cases had IM in the portion of the surgical specimen proximal to the primary tumor, 11 cases had IM in the distal portion, and 7 cases had IM on both sides. Nine cases had IM in an adjacent organ, 6 cases had IM in the esophageal wall, and 3 cases had IM in the duodenal wall.

Prognosis of the IM cases

The median survival time for all gastric cancers with IM was 11 months (with a 13.9 % survival rate at 3 years). Survival time was 13.5 months (with an 18.8 % survival rate at 3 years) for cases in which R0 resection was obtained, and 7.5 months (with an 8.9 % survival rate at 3 years) for cases in which R1/2 resection was obtained, with no significant difference observed between the two groups ($p = 0.12$) (Fig. 2). However, no cases of recurrence were observed in 5 of 14 cases in which R0 resection was obtained.The median survival time for all gastric cancers with IM was significantly lower than for cases of advanced gastric cancer without IM ($p < 0.0001$). In cases of advanced gastric cancer without IM, the median survival time was 39.4 months with a 51.1 % survival rate at 3 years (Fig. 3).

Prognosis by distance from the primary lesion and by the size of the IM was also calculated. The relationship between the size of the IM and the distance from the primary lesion is shown in Fig. 4. A constant tendency was not observed between the IM size and the distance from the primary lesion, but the IM size was approximately within 2 cm, and many occurred within 2 cm of the primary lesion. Thus, when the cutoff value for the distance was set at various lengths from 0.5 to 2 cm, the 1-cm distance was associated with the most significant difference in survival. Cases with a distance from the primary tumor of less than 1 cm lived significantly longer than cases with a distance of 1 cm or more from the primary tumor. In all cases of IM for the distance from the primary tumor, 3-year survival rates and median survival times were 25.7 % and 28 months versus 0 % and 8 months ($p = 0.0026$), respectively. In R0 cases of IM for the distance from the primary tumor, 3-year survival rates and median survival times were 41.7 % and 29 months versus 0 % and 11 months, respectively ($p = 0.0075$) (Fig. 5).

Three-year survival rates and median survival times of cases with an IM size smaller than 1 cm were higher than those of cases with IMs of 1 cm or larger, although the difference was not significant. In all cases of IM for the IM size, 3-year survival rates and median survival times were 22.1 % and 13 months versus 0 % and 9 months, respectively ($p = 0.36$). In R0 cases of IM for IM size, 3-year survival rates and median survival times were 20.0 % and 14.5 months versus not assessable and 11.5 months, respectively ($p = 0.72$) (Fig. 6).

Table 2 Characteristics of intramural metastasis (IM)

Size (cm)	
Mean ± SD (range)	1.09 ± 1.10 (0.2–6.0)
Number of IM	
1/2/3/4/≥5	18/4/4/1/2
Affected layer of IM	
sm/mp/ss/se	13/10/5/1
Distance from primary tumor (cm)	
Mean ± SD (range)	1.21 ± 0.94 (1–5.5)
Preoperative diagnosis (%)	5 (17.2)
Direction from primary tumor	
Anal/oral/both sides	11/11/7
Located in an adjacent organ esophagus/ duodenum	3/6

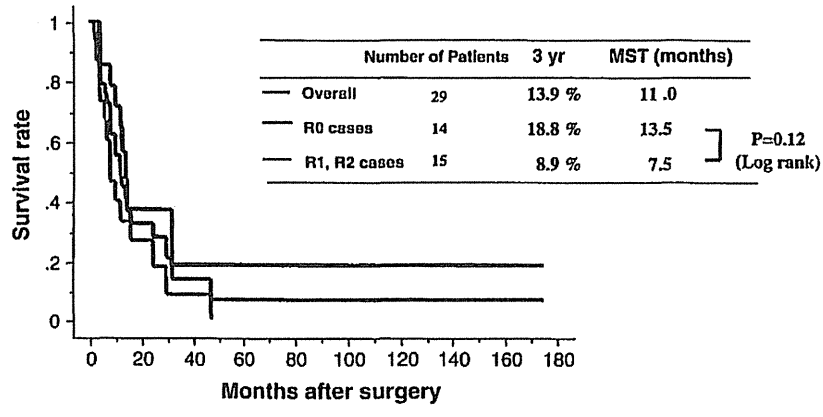

Fig. 2 Postoperative survival of IM cases. *3 yr* 3-year survival rate, *MST* mean survival time

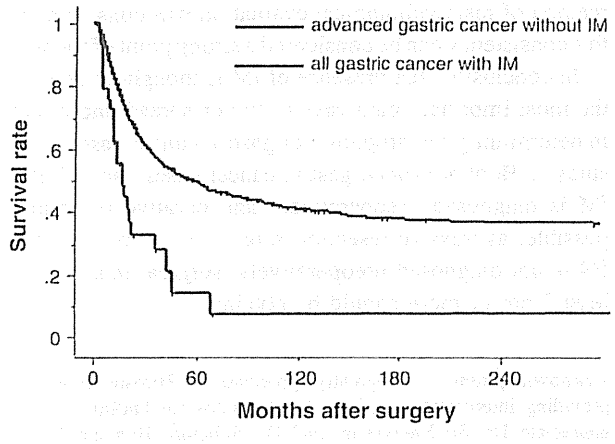

Fig. 3 Survival curves for patients with all gastric cancers with IM (*blue line*, $n = 29$) and advanced gastric cancer without IM (*red line*, $n = 2{,}770$): $p < 0.0001$

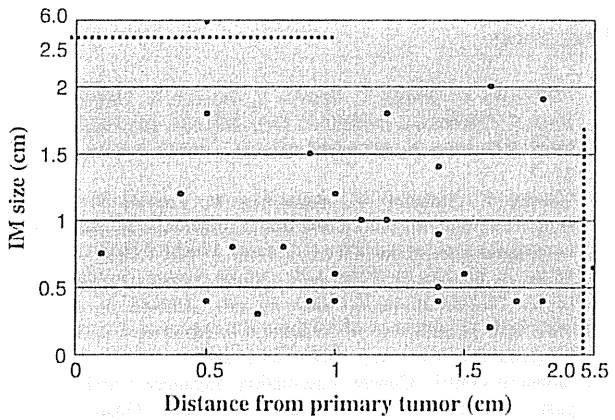

Fig. 4 Correlation between size of IM and distance from primary tumor. The majority of IMs were less than 2 cm in size and were located within 2 cm of the primary tumor

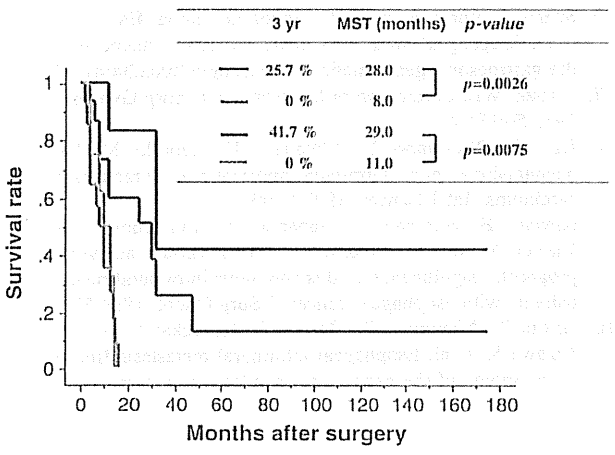

Fig. 5 Postoperative survival according to distance from primary tumor. *Red line* (15 patients): <1 cm from the primary tumor of all cases, *orange line* (14 patients): ≥1 cm from the primary tumor of all cases, *blue line* (6 patients): <1 cm from the primary tumor of R0 cases, *green line* (8 patients): ≥1 cm from the primary tumor of R0 cases

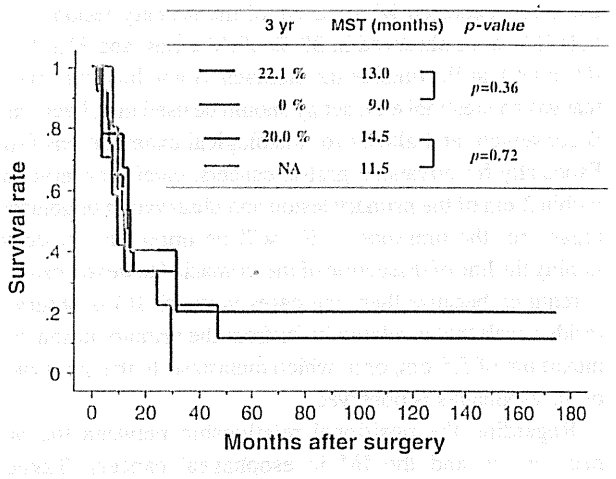

Fig. 6 Postoperative survival according to size of IM. *Red line* (17 patients): <1 cm in size (all cases), *orange line* (12 patients): ≥1 cm in size (all cases), *blue line* (6 patients): <1cm in size of R0 cases, *green line* (8 patients): ≥1 cm in size of R0 cases. *NA* not assessable

Discussion

Generally, IM in gastric adenocarcinoma is very rare. A PubMed search from 1950 to 2010 using gastric cancer and IM as keywords revealed only three case reports [5, 6], and there are no articles to date that have verified this condition. This study provided the first analysis of IM in gastric cancer.

In contrast to IM in gastric cancer, IM is often observed in esophageal squamous cell carcinoma and was first reported by Watson in 1933 [7]. The frequency reportedly ranges from 10.8 to 15.5 % in advanced esophageal cancers [2, 3, 8, 9]. In this study, the incidence of IM was only 0.6 % in cases of resected gastric cancer and 1 % in advanced cancer cases, and it was a very rare pathology, compared with the incidence in esophageal cancer.

Compared with primary lesions without IM in esophageal squamous cell carcinoma, the clinicopathological features of primary lesions with IM are reported to include advanced stage grouping, a higher rate of lymph node metastasis (79–99 %), and a higher rate of capillary invasion (76–100 %) [1–3, 9], features that correspond to the results of this study in gastric cancer. Distant metastasis was detected in 37.9 % of IM in this study, whereas the reported rate of IM is 29.2 % in esophageal cancer [2].

It is believed that IM in esophageal cancer is mediated by lymphatic invasion to the submucosal layer. Consequently, it is believed that lymphatic invasion and/or lymph node metastasis cases are common, with large numbers of lymph node metastases [7]. In this study, based on the fact that cases positive for capillary invasion are common, particularly for lymphatic invasion, the proliferation of cancer cells deeper than the submucosal layer via lymph

flow was also assumed to be an onset mechanism for IM in gastric cancer, similar to esophageal cancer.

In this study, the IM size was approximately within 2 cm, and many occurred within 2 cm of the primary lesion. Multiple IMs were observed in 38 % of IM cases, and 31.0 % of IM cases had IM outside the stomach. Some literature states that gastrointestinal endoscopy should be used first, because it is convenient and allows for histological examinations [10]. Especially for advanced gastric cancers, careful observation within 2 cm of the primary lesion and observation of adjacent organs for the presence of IM will be important for determining the line of dissection of the stomach. However, caution is required because there are cases in which IM is observed inside a wall that is relatively far from the primary lesion, at a maximum of 5.5 cm, or in which metastasis to the duodenum or the esophagus is observed.

Regarding the positional relationship between the primary lesion and the IM in esophageal cancers, Takubo et al. [2] reported that IM was equally present on both sides of the primary lesion. Similarly, in our study, IM was present equally on both sides.

In this study, the IM was detected preoperatively in five cases (17.2 %). All IMs existed in layers deeper than the sm, so submucosal tumors covered with normal epithelium are an important finding in gastrointestinal barium studies and endoscopic examinations. Takubo et al. [2] reported that the IM in esophageal cancer was detected preoperatively 54.2 % of the time, with a dome-like appearance covered with normal epithelium, similar to that of submucosal tumors, often with erosion or ulceration. The difficulties in making a preoperative diagnosis of IM in gastric cancer probably result from the small size and the absence of erosion and ulceration.

The prognosis of esophageal cancer accompanied by IM is exceedingly poor, with a survival rate at 5 years of 9 % and a median survival time of 7 months [3], making it one of the major causes of poor postoperative prognosis [1, 2]. The median survival time of gastric cancer cases with IM was relatively favorable, at 11 months (13.9 % survival rate at 3 years). However, the results of our study indicated a significantly poorer prognosis in all gastric cancers with IM than in cases of advanced gastric cancer without IM. A subgroup of cases with IM within 1 cm of the primary lesion had a relatively favorable prognosis in this study. Yuasa et al. [3] also reported that a subgroup of cases with IM less than 2.0 cm from the primary tumor may have a relatively favorable prognosis in esophageal cancer. More specifically, even if a gastric cancer is accompanied by IM, long-term survival may be achieved if curability can be obtained and if the IM remains in the vicinity of the primary lesion.

This study has several limitations. Because of the low overall number of cases diagnosed with IM in gastric cancer, the number of cases in our study was too small to perform more rigorous statistical evaluation, and bias may have affected the clinicopathological investigation. However, the method of histopathological evaluation was consistent, and this consistency can be considered a strong point of the study.

In conclusion, the presence of IM is thought to be one of the most important pathways of tumor spread and a factor in determining the prognosis of gastric cancer cases. In this study, 1 % of advanced gastric cancer cases had IM. If the IM is diagnosed preoperatively and curative resection is possible, aggressive resection should be performed. If the IM is not diagnosed preoperatively, surgical margins of at least 2 cm or more should be obtained.

Acknowledgments We greatly appreciate Dr. Hiroshi Kawachi for providing interpretations of the histopathological findings. We also appreciate Dr. So Katayanagi and Dr. Seiichiro Hoshino for their writing assistance.

Conflict of interest None.

References

1. Nishimaki T, Suzuki T, Tanaka Y, Aizawa K, Hatakeyama K, Muto T. Intramural metastases from thoracic esophageal cancer: local indicators of advanced disease. World J Surg. 1996;20: 32–7.
2. Takubo K, Sasajima K, Yamashita K, Tanaka Y, Fujita K. Prognostic significance of intramural metastasis in patients with esophageal carcinoma. Cancer (Phila). 1990;65:1816–9.
3. Yuasa N, Miyake H, Yamada T, Oda K, Nimura Y, Nagasaka T, et al. Prognostic significance of the location of intramural metastasis in patients with esophageal squamous cell carcinoma. Langenbecks Arch Surg. 2004;389:122–7.
4. Japanese Gastric Cancer Association. Japanese classification of gastric carcinoma: 3rd English edition. Gastric Cancer 2011;14:101–112.
5. Ikeda O, Toh Y, Aoki Y, Harimoto N, Taomoto J, Masuda T, et al. Multiple and metachronous esophageal intramural metastases from a gastric adenocarcinoma. Gastric Cancer. 2008;11: 119–22.
6. Szanto I, Voros A, Nagy P, Gonda G, Gamal EM, Altorjay A, et al. Esophageal intramural metastasis from adenocarcinoma of the gastroesophageal junction. Endoscopy. 2002;34:418–20.
7. Watson WL. Carcinoma of the esophagus. Surg Gynecol Obstet. 1933;56:884–97.
8. Kato H, Tachimori Y, Watanabe H, Itabashi M, Hirota T, Yamaguchi H, et al. Intramural metastasis of thoracic esophageal carcinoma. Int J Cancer. 1992;50:49–52.
9. Kuwano H, Watanabe M, Sadanaga N, Kamakura T, Nozoe T, Yasuda M, et al. Univariate and multivariate analyses of the prognostic significance of discontinuous intramural metastasis in patients with esophageal cancer. J Surg Oncol. 1994;57:17–21.
10. Hirota T, Nishimaki T, Suzuki T, Komukai S, Kuwabara S, Aizawa K, et al. Esophageal intramural metastasis from an adenocarcinoma of the gastric cardia: report of a case. Surg Today. 1998;28:1160–2.

Transplant Infectious Disease, ISSN 1398-2273

Acute kidney injury after myeloablative cord blood transplantation in adults: the efficacy of strict monitoring of vancomycin serum trough concentrations

H. Mae, J. Ooi, S. Takahashi, S. Kato, T. Kawakita, Y. Ebihara, K. Tsuji, F. Nagamura, H. Echizen, A. Tojo. Acute kidney injury after myeloablative cord blood transplantation in adults: the efficacy of strict monitoring of vancomycin serum trough concentrations. Transpl Infect Dis 2013: **15**: 181–186. All rights reserved

Abstract: *Background.* Acute kidney injury (AKI) is a common medical complication after myeloablative allogeneic stem cell transplantation (SCT). We have previously performed a retrospective analysis of AKI after cord blood transplantation (CBT) in adults, and found that the maximum of vancomycin (VCM) trough levels were significantly higher in patients with AKI. Following these results, we have monitored VCM serum trough concentrations more strictly, to not exceed 10.0 mg/L, since 2008.
Methods. In this report, we performed an analysis of AKI in a new group of 38 adult patients with hematological malignancies treated with unrelated CBT after myeloablative conditioning between January 2008 and July 2011.
Results. Cumulative incidence of AKI at day 100 after CBT was 34% (95% confidence interval 19–50). The median of the maximum value of VCM trough was 8.8 (4.5–12.2) mg/L. In multivariate analysis, no factor was associated with the incidence of AKI. No transplant-related mortality was observed. The probability of disease-free survival at 2 years was 83%.
Conclusion. These findings suggest that strict monitoring of VCM serum trough concentrations has a beneficial effect on outcomes of CBT.

H. Mae[1], J. Ooi[2], S. Takahashi[2], S. Kato[2], T. Kawakita[2], Y. Ebihara[3], K. Tsuji[3], F. Nagamura[2], H. Echizen[4], A. Tojo[2]

[1]Department of Pharmacy, Institute of Medical Science, University of Tokyo, Tokyo, Japan, [2]Department of Hematology and Oncology, Institute of Medical Science, University of Tokyo, Tokyo, Japan, [3]Department of Pediatric Hematology and Oncology, Institute of Medical Science, University of Tokyo, Tokyo, Japan, [4]Department of Pharmacotherapy, Meiji Pharmaceutical University, Tokyo, Japan

Key words: vancomycin; myeloablative conditioning; cord blood transplantation; acute kidney injury

Correspondence to:
Jun Ooi, MD, Department of Hematology and Oncology, Institute of Medical Science, University of Tokyo, 4-6-1 Shirokanedai, Minato-ku, Tokyo 108-8639, Japan
Tel: +81 3 5449 5543
Fax: +81 3 5449 5429
E-mail: jun-ooi@ims.u-tokyo.ac.jp

Received 14 May 2012, revised 17 July 2012, 13 August 2012, accepted for publication 18 August 2012

DOI: 10.1111/tid.12038
Transpl Infect Dis 2013: **15**: 181–186

Acute kidney injury (AKI) is a common medical complication early after myeloablative allogeneic stem cell transplantation (SCT). The incidence of AKI, defined as a 2-fold rise in serum creatinine (sCr) concentration from baseline, has been reported ranging from 36% to 72% in SCT in a myeloablative setting (1–7), and about 20% required hemodialysis. We have previously reported a retrospective analysis of AKI in a group of 54 adult patients with hematological malignancies who received unrelated cord blood transplantation (CBT) after myeloablative conditioning between 2004 and 2007 (8). A statistically significant decrement of renal function from baseline was observed between days 11 and 20. Among the 54 patients, AKI occurred in 27.8% and was associated with a high mortality rate. Although no difference was seen in maximum cyclosporine (CYA) trough levels, the maximum vancomycin (VCM) trough levels were significantly higher in patients with AKI (8). Following these results, we have monitored VCM serum trough concentrations more strictly. In this report, we performed an analysis of AKI in a new group of 38 adult patients with hematological malignancies treated with unrelated CBT after myeloablative conditioning between January 2008 and

July 2011. The main purpose of this retrospective single-center study was to confirm the efficacy of strict monitoring of VCM serum trough concentrations, as well as to identify factors related to the incidence of AKI.

Patients and methods

Patients

This was a retrospective single-center analysis. Between January 2008 and July 2011, 39 consecutive adult patients with hematological malignancies were treated with unrelated CBT at The Institute of Medical Science, University of Tokyo. We excluded 1 patient who experienced primary engraftment failure. A total of 38 patients were analyzed. Patients qualified as standard risk if they were in first or second complete remission, had chronic-phase chronic myelogenous leukemia or refractory anemia of myelodysplastic syndrome, or had no high-risk cytogenetics. Patients in third complete remission, in relapse, or in refractory disease, with chronic myelogenous leukemia beyond chronic phase, or with high-risk cytogenetics were classified as high risk. Analyses of data were performed in December 2011. Written informed consent for treatment was obtained from all patients.

Conditioning

All patients received 4 fractionated 12 Gy total body irradiation on days −8 and −7, in addition to cytosine arabinoside (Ara-C) and cyclophosphamide. Ara-C was administered intravenously (IV) over 2 h at a dose of 3 g/m^2 every 12 h on day −5 and −4 (total dose 12 g/m^2). In patients with myeloid malignancies, recombinant human granulocyte colony-stimulating factor (G-CSF) was combined with Ara-C. G-CSF was administered by continuous infusion at a dose of 5 μg/kg/day. Infusion of G-CSF was started 12 h before the first dose of Ara-C and stopped at the completion of the last dose. Cyclophosphamide was administered IV over 2 h at a dose of 60 mg/kg once daily on days −3 and −2 (total dose 120 mg/kg). Two days after the completion of conditioning, patients received a CBT.

Graft-versus-host disease (GVHD) prophylaxis

All patients received standard CYA and methotrexate as GVHD prophylaxis. CYA was given IV every day starting on day −1 at a dose of 3 mg/kg/day. Methotrexate (15 mg/m^2 IV) was given on day 1, and 10 mg/m^2 on day 3 and 6. Once oral intake could be tolerated, patients were administered oral CYA at a dose of 1:2, in 2 divided doses per day, based on the last intravenous dose. CYA was reduced when sCr levels rose above 1.5 times baseline, or other serious agent-associated toxicities occurred. Physicians could freely modify the CYA dose for patients experiencing severe acute GVHD (aGVHD) or risk of disease relapse. Corticosteroid-based treatment was considered when grade II or higher severe aGVHD occurred (0.5–2 mg/kg).

Supportive care

All patients received G-CSF by intravenous infusion starting on day 1 until durable granulocyte recovery was achieved. The supportive care regimen, including prophylaxis for infection was the same as previously reported (8, 9).

Monitoring

All patients were monitored retrospectively 10 days before, and after the first 100 days, of CBT. Daily laboratory data collecting and the detecting method of VCM and CYA trough concentration were the same as previously reported (8). Therapeutic drug monitoring for VCM by assessing serum trough concentration was done twice in weekly, and modified to not exceed 10.0 mg/L.

End-points and definitions

AKI was defined as 2-fold rise in sCr concentration on daily laboratory results from the baseline (the average of days −10 to 0). Myeloid engraftment was defined as the first of 3 consecutive days, during which the absolute neutrophil count was at least 0.5 × 10^9/L. Platelet recovery time was achieved on the first of 3 days when the platelet count was higher than 50 × 10^9/L without transfusion support. The aGVHD was graded according to previously published criteria (10). Transplant-related mortality was defined as death from any cause except relapse. Relapse was defined by morphologic evidence of disease in peripheral blood, bone marrow, or extramedullary sites. Disease-free survival was defined as the time from CBT to relapse, death, or the last observation.

Statistical analysis

Continuous variables are expressed as median and their range. For dichotomous variables, the frequencies of positive occurrence are given along with their corresponding percentages. Continuous variables were divided into high or low with their median values, and a single VCM trough concentration of 10.0 mg/L was defined as a threshold level for analysis. Cumulative incidence of AKI was estimated with competing risk setting, of which death and relapse were defined as competing risk events. Variables considered in univariate analysis were body weight, age, recipient gender, recipient cytomegalovirus serology, disease status at transplant (standard or high risk), total nucleated cell dose, CD34+ cell dose, baseline sCr levels, VCM use, VCM trough levels, CYA trough levels, foscarnet use, aminoglycosides use, days of neutrophil engraftment, aGVHD grade 3–4, and positive blood culture result. Variables with a *P*-value <0.1 for cumulative incidence of AKI were tested in multivariate analysis using Cox proportional hazards models, and *P*-values <0.05 were considered to be statistically significant. The probability of disease-free survival was estimated from the time of CBT according to the Kaplan–Meier method. Endpoints were calculated at the last contact, the date of the last follow-up being December 1, 2011. Statistical software R, version 2.12.2, was used for analysis.

Results

Characteristics of patients and cord blood units

The characteristics of 38 patients and cord blood units are shown in Table 1. Among the patients, the median age was 41.5 years (range, 18–52 years), the median weight was 59.5 kg (range, 39–76 kg), the median number of cryopreserved nucleated cells was 2.8×10^7/kg (range, $1.7–5.7 \times 10^7$/kg), and the median number of cryopreserved CD34+ cells was 0.9×10^5/kg (range, $0.4–2.6 \times 10^5$/kg). All patients received a single and human leukocyte antigen-mismatched cord blood unit.

Time courses of changing renal function

No patient had confirmed renal dysfunction before transplantation. The changes of renal function as variations (%) of sCr from baseline levels observed on days 11–20 were greatest and significant (+15.8%,

Characteristics and clinical course

Characteristics	
Patients, *n*	38
Male/Female, *n*	25/13
Median age, years (range)	41.5 (18–52)
Median weight, kg (range)	59.5 (39–76)
Median number of cryopreserved nucleated cells, $\times 10^7$/kg (range)	2.8 (1.7–5.7)
Median number of cryopreserved CD34+ cells, $\times 10^5$/kg (range)	0.9 (0.4–2.6)
Recipient CMV status, Positive/Negative, *n*	32/6
Diagnosis	
AML, *n*	12
MDS-related secondary AML, *n*	6
RAEB, *n*	3
RA, *n*	2
CML, *n*	3
ALL, *n*	11
NHL, *n*	1
Disease status at transplant	
Standard risk, *n*	10
High risk, *n*	28
Conditioning regimen	
TBI + Ara-C/G-CSF + CY, *n*	26
TBI + Ara-C + CY, *n*	12
GVHD prophylaxis	
CYA + MTX, *n*	38
Baseline sCr, mg/dL (range)	0.62 (0.33–0.87)
Neutrophil >0.5 × 10^9/L, days (range)	21 (17–30)
Patients with positive blood culture, *n* (%)	6 (16)
Patients taking aminoglycosides, *n* (%)	32 (84)
Patients taking foscarnet, *n* (%)	10 (26)
Patients taking liposomal amphotericin, *n* (%)	16 (42)
Maximum CYA trough value, μg/L (range)	258.5 (40–453)
Patients taking VCM, *n* (%)	32 (84)
Duration of VCM therapy, days (range)	54 (6–100)
Maximum VCM trough value, mg/L (range)	8.8 (5.2–12.2)
Patients with maximum VCM trough value, >10.0 mg/L, *n* (%)	9 (24)
Patient requiring hemodialysis, *n* (%)	0 (0)

CMV, cytomegalovirus; AML, acute myelogenous leukemia; MDS, myelodysplastic syndrome; RAEB, refractory anemia with excess blasts; RA, refractory anemia; CML, chronic myelogenous leukemia; ALL, acute lymphoblastic leukemia; NHL, non-Hodgkin's lymphoma; TBI, total body irradiation; Ara-C, cytosine arabinoside; G-CSF, recombinant human granulocyte colony-stimulating factor; CY, cyclophosphamide; GVHD, graft-versus-host disease; CYA, cyclosporine; MTX, methotrexate; sCr, serum creatinine; VCM, vancomycin.

Table 1

0.57 ± 0.18 mg/dL to 0.71 ± 0.24 mg/dL, $P < 0.001$). No obvious recovery occurred of declined renal function, which remained until day 100.

Incidence and risk factors of AKI

Cumulative incidence of AKI at day 100 after CBT was 34% (95% CI 19–50) (Fig. 1). The median of the maximum value of VCM trough was 8.8 (4.5–12.2) mg/L. In univariate analysis, baseline sCr levels and foscarnet use were associated with the incidence of AKI (Table 2). In multivariate analysis, no factor was associated with the incidence of AKI (Table 2).

Transplant outcomes

All patients had myeloid reconstitution, and the median time to >0.5 × 10^9/L absolute neutrophil count was 21 days (range, 17–30 days). A self-sustained platelet count >50 × 10^9/L was achieved in 37 patients at a median time of 45.5 days (range, 34–127 days). In 37 of 38 evaluable patients, aGVHD occurred. The grading of aGVHD was grade I in 7 patients, grade II in 25, grade III in 4, and grade IV in 1. No one experienced hepatic veno-occlusive disease. Six of 38 patients (16%) had positive blood culture; however, no one had confirmed hypotension, indicated with decrease in systolic blood pressure >10 mmHg to <90 mmHg. Of 6 patients with positive blood cultures, 4 patients were not administered VCM. The total number of positive blood cultures was 13 of 998 specimens. Ten of 13 bacterial pathogens from blood cultures were gram-positive cocci (Table 3). Vancomycin-resistant *Enterococci* were detected in 1 patient from blood culture, however, this had been continuously detected from stool specimens since admission. No patients required hemodialysis. Among the 38 patients, no patient died of transplant-related causes (transplant-related mortality 0%). Six patients relapsed. Of these 6 patients, 5 patients died of relapse. A total of 32 of 38 patients are alive and free of disease at between 139 and 1400 days (median: 634 days) after CBT. The probability of disease-free survival at 2 years was 83% and 77% at 3 years (Fig. 2).

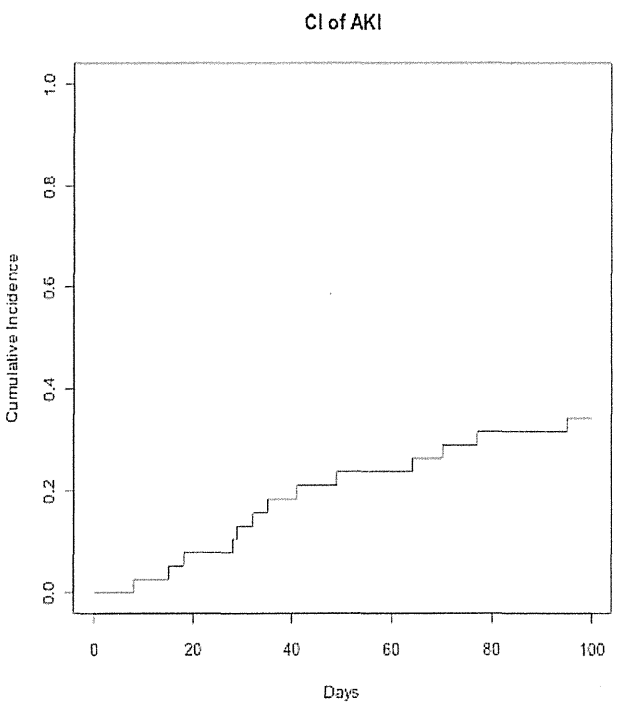

Fig. 1. Cumulative incidence (CI) of acute kidney injury (AKI).

Discussion

In this study, similar trends were observed in the time course of renal function changes as previously reported (8). However, the elevation in sCr was lower in this study, especially in days 11–20 (from 35.0% [8] to 15.8% in this study). Cumulative incidence of AKI was 34%; however, this was not assessed in our previous study (8). When we assessed the incidence of AKI with an identical definition to the previous

Univariate and multivariate analysis of factors associated with acute kidney injury

	Univariate analysis		Multivariate analysis	
	Hazard ratio (95% CI)	*P*	Hazard ratio (95% CI)	*P*
Baseline sCr, mg/dL				
>0.62	0.27 (0.08–0.98)	0.047	0.33 (0.08–1.32)	0.12
<0.62	1		1	
Foscarnet				
(+)	3.11 (1.07–9.05)	0.037	2.45 (0.71–8.42)	0.15
(−)	1		1	
VCM trough, >10.0 mg/L				
(+)	2.68 (0.89–8.09)	0.081	2.64 (0.76–9.19)	0.13
(−)	1		1	

CI, confidence interval; sCr, serum creatinine; VCM, vancomycin.

Table 2

Isolated bacterial pathogens from blood cultures

Pathogens	*n*
Enterococcus faecalis	3
Vancomycin-resistant *Enterococcus faecium*	3
Methicillin-resistant *Staphylococcus* species	1
Methicillin-resistant *Staphylococcus epidermidis*	3
Stenotrophomonas maltophilia	1
Bacillus species	1
Bacillus cereus	1

Table 3

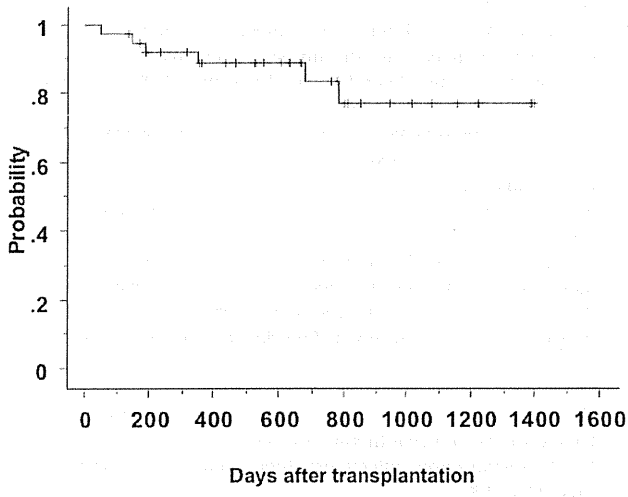

Fig. 2. Probability of disease-free survival after cord blood transplantation.

study, defined as just a 2-fold rise in sCr of 10 days average before and after transplantation, the incidence of AKI decreased to 11% in this study. In our previous study, the maximum VCM trough levels were significantly higher in patients with AKI (8); therefore, we have monitored VCM serum trough concentrations more strictly to not exceed 10.0 mg/L since 2008 in this study period. The average maximum value of VCM trough levels was lowered to 8.7 ± 2.1 mg/L from 12.2 ± 4.6 mg/L in the previous study, and proportion of patients with trough levels >10.0 mg/L was also decreased from 57% to 24%. Although baseline sCr levels and foscarnet use were associated with the incidence of AKI, VCM trough levels were not associated with AKI in univariate analysis. No factor was associated with AKI in multivariate analysis. Parikh et al. (11) reported AKI significantly affects survival after myeloablative allogeneic SCT in their meta-analysis, and more recently, Kagoya et al. (7) as well as Gooley et al. (12) reported the association of severity of AKI classification and non-relapse mortality within 100 days after transplantation. Although cumulative incidence of AKI was 34% in this study, no patients required hemodialysis or died of transplant-related causes. Recently, Yazaki et al. (13) reported the association of overall mortality and early bacterial infection of CBT in adults. They reported that cumulative incidence of early bacterial infection at day 100 was 21%, early bacterial infection had a negative effect on survival for adults, and the median day of development was 10 days after transplant, suggesting that prevention of bacterial infection in the very early post-CBT phase is important. Recently, a shift has occurred in the type of infecting organisms that cause bacteremia from predominantly gram-negative organisms to gram-positive cocci. The same trend is confirmed in the CBT (13, 14). VCM has an important role for infection control of gram-positive bacteremia, and was given to almost all the patients in this study. The reduced susceptibility of staphylococci for VCM has been reported since the mid 1990s, and prolonged exposure to lower VCM concentration has been associated with resistance (15). Although very few studies about pharmacokinetics and pharmacodynamics of VCM are available, several studies revealed area under the curve/minimum inhibitory concentration (AUC/MIC) as a preferred parameter, and AUC/MIC >400 associated with successful outcome and prevention of resistance (15, 16). Because of the difficulty of determining multiple concentrations for calculating AUC in the clinical setting, VCM trough concentrations have been recommended as the best surrogate marker for AUC/MIC, and concentrations of 15–20 mg/L – higher than the 5–15 mg/L previously recommended – is recommended as the target range (16). However, because an increased risk of nephrotoxicity with elevated VCM trough concentrations has been reported, and no appropriate pharmacokinetic/pharmacodynamic parameters for VCM have been determined (15, 17, 18), careful assessments are needed for using VCM at high target concentrations. Although we controlled VCM levels to not exceed 10.0 mg/L in this study, no patient died of bacterial infections. Further studies are required to determine the optimal VCM trough concentrations. Few reports are available about monitoring VCM trough concentrations for preventing AKI in allogeneic SCT in adults. Despite the limitations associated with this retrospective review of a small number of patients, our results suggest that strict monitoring of VCM serum trough concentrations has a beneficial effect on outcomes of CBT.

Acknowledgements:

Thanks: The authors would like to thank the physicians and nurses who cared for patients in this study.

Conflict of interest: The authors declare no conflict of interest of this manuscript.

Author contributions: H.M. and J.O. designed the study, analyzed data, and wrote the manuscript; J.O., S.T., S.K., T.K., Y.E., K.T., and A.T. cared for the patients; F.N. performed the statistical analysis; and H.E. and A.T. reviewed the study.

References

1. Zager RA, O'Quigley J, Zager BK, et al. Acute renal failure following bone marrow transplantation: a retrospective study of 272 patients. Am J Kidney Dis 1989; 13: 210–216.
2. Gruss E, Bernis C, Tomas JF, et al. Acute renal failure in patients following bone marrow transplantation: prevalence, risk factors and outcome. Am J Nephrol 1995; 15: 473–479.
3. Parikh CR, McSweeney PA, Korular D, et al. Renal dysfunction in allogeneic hematopoietic cell transplantation. Kidney Int 2002; 62: 566–573.
4. Parikh CR, Schrier RW, Storer B, et al. Comparison of ARF after myeloablative and nonmyeloablative hematopoietic cell transplantation. Am J Kidney Dis 2005; 45: 502–509.
5. Hingorani SR, Guthrie K, Batchelder A, et al. Acute renal failure after myeloablative hematopoietic cell transplant: incidence and risk factors. Kidney Int 2005; 67: 272–277.
6. Caliskan Y, Besisik SK, Sargin D, Ecder T. Early renal injury after myeloablative allogeneic and autologous hematopoietic cell transplantation. Bone Marrow Transplant 2006; 38: 141–147.
7. Kagoya Y, Kataoka K, Nannya Y, Kurokawa M. Pretransplant predictors and posttransplant sequels of acute kidney injury after allogeneic stem cell transplantation. Biol Blood Marrow Transplant 2011; 17: 394–400.
8. Mae H, Ooi J, Takahashi S, et al. Early renal injury after myeloablative cord blood transplantation in adults. Leuk Lymphoma 2008; 49: 538–542.
9. Takahashi S, Iseki T, Ooi J, et al. Single-institute comparative analysis of unrelated bone marrow transplantation and cord blood transplantation for adult patients with hematologic malignancies. Blood 2004; 104: 3813–3820.
10. Przepiorka D, Weisdorf D, Martin P, et al. 1994 Consensus Conference on Acute GVHD Grading. Bone Marrow Transplant 1995; 15: 825–828.
11. Parikh CR, McSweeney P, Schrier RW. Acute renal failure independently predicts mortality after myeloablative allogeneic hematopoietic cell transplant. Kidney Int 2005; 67: 1999–2005.
12. Gooley TA, Chien JW, Pergam SA, et al. Reduced mortality after allogeneic hematopoietic-cell transplantation. N Engl J Med 2010; 363: 2091–2101.
13. Yazaki M, Atsuta Y, Kato K, et al. Incidence and risk factors of early bacterial infections after unrelated cord blood transplantation. Biol Blood Marrow Transplant 2009; 15: 439–446.
14. Tomonari A, Takahashi S, Ooi J, et al. Bacterial bloodstream infection in neutropenic adult patients after myeloablative cord blood transplantation: experience of a single institution in Japan. Int J Hematol 2007; 85: 238–241.
15. Rybak MJ. The pharmacokinetic and pharmacodynamic properties of vancomycin. Clin Infect Dis 2006; 42: S35–S39.
16. Rybak M, Lomaestro B, Rotschafer JC, et al. Therapeutic monitoring of vancomycin in adult patients: a consensus review of the American Society of Health-System Pharmacists, the Infectious Diseases Society of America, and the Society of Infectious Diseases Pharmacists. Am J Health Syst Pharm 2009; 66: 82–98.
17. Hidayat LK, Hsu DI, Quist R, Shriner KA, Wong-Beringer A. High-dose vancomycin therapy for methicillin-resistant *Staphylococcus aureus* infections: efficacy and toxicity. Arch Intern Med 2006; 166: 2138–2144.
18. Pritchard L, Baker C, Leggett J, Sehdev P, Brown A, Bayley KB. Increasing vancomycin serum trough concentrations and incidence of nephrotoxicity. Am J Med 2010; 123: 1143–1149.

OPEN ACCESS Freely available online

PLOS | ONE

Overexpression of Cohesion Establishment Factor DSCC1 through E2F in Colorectal Cancer

Kiyoshi Yamaguchi[1]*, Rui Yamaguchi[2], Norihiko Takahashi[1], Tsuneo Ikenoue[1], Tomoaki Fujii[1], Masaru Shinozaki[3], Giichiro Tsurita[3], Keisuke Hata[3], Atsushi Niida[4], Seiya Imoto[4], Satoru Miyano[2,4], Yusuke Nakamura[5], Yoichi Furukawa[1]

1 Division of Clinical Genome Research, Advanced Clinical Research Center, Institute of Medical Science, The University of Tokyo, Tokyo, Japan, **2** Laboratory of Sequence Analysis, Human Genome Center, Institute of Medical Science, The University of Tokyo, Tokyo, Japan, **3** Department of Surgery, Research Hospital, Institute of Medical Science, The University of Tokyo, Tokyo, Japan, **4** Laboratory of DNA Information Analysis, Human Genome Center, Institute of Medical Science, The University of Tokyo, Tokyo, Japan, **5** Laboratory of Molecular Medicine, Human Genome Center, Institute of Medical Science, The University of Tokyo, Tokyo, Japan

Abstract

Ctf18-replication factor C complex including Dscc1 (DNA replication and sister chromatid cohesion 1) is implicated in sister chromatid cohesion, DNA replication, and genome stability in *S. cerevisiae* and *C. elegans*. We previously performed gene expression profiling in primary colorectal cancer cells in order to identify novel molecular targets for the treatment of colorectal cancer. A feature of the cancer-associated transcriptional signature revealed from this effort is the elevated expression of the proto-oncogene *DSCC1*. Here, we have interrogated the molecular basis for deviant expression of human DSCC1 in colorectal cancer and its ability to promote survival of cancer cells. Quantitative PCR and immunohistochemical analyses corroborated that the expression level of DSCC1 is elevated in 60–70% of colorectal tumors compared to their matched noncancerous colonic mucosa. An *in silico* evaluation of the presumptive *DSCC1* promoter region for consensus DNA transcriptional regulatory elements revealed a potential role for the E2F family of DNA-binding proteins in controlling DSCC1 expression. RNAi-mediated reduction of E2F1 reduced expression of DSCC1 in colorectal cancer cells. Gain- and loss-of-function experiments demonstrated that DSCC1 is involved in the viability of cancer cells in response to genotoxic stimuli. We reveal that E2F-dependent expression of DSCC1 confers anti-apoptotic properties in colorectal cancer cells, and that its suppression may be a useful option for the treatment of colorectal cancer.

Citation: Yamaguchi K, Yamaguchi R, Takahashi N, Ikenoue T, Fujii T, et al. (2014) Overexpression of Cohesion Establishment Factor DSCC1 through E2F in Colorectal Cancer. PLoS ONE 9(1): e85750. doi:10.1371/journal.pone.0085750

Editor: Srikumar P. Chellappan, H. Lee Moffitt Cancer Center & Research Institute, United States of America

Received October 28, 2013; **Accepted** November 30, 2013; **Published** January 17, 2014

Funding: This work was supported in part by Grant-in-Aid for Young Scientists (#23790126), MEXT/JSPS, Japan to K. Yamaguchi, and Global COE Program "Center of education and research for the advanced genome-based medicine for personalized medicine and the control of worldwide infectious diseases", MEXT/Japan Society for the Promotion of Science, Japan to Y. Furukawa. The funders had no role in study design, data collection and analysis, decision to publish, or preparation of the manuscript.

Competing Interests: The authors have declared that no competing interests exist.

* E-mail: kiyamagu@ims.u-tokyo.ac.jp

Introduction

Colorectal cancer (CRC) is one of the most frequent human neoplasms in the world. In CRC cells, disruption of systems governing genetic or epigenetic integrity renders different features such as chromosomal instability (CIN), microsatellite instability (MSI), and CpG island methylator phenotype (CIMP). A great majority of colorectal tumors exhibit CIN that includes gross genetic changes such as deletions, amplifications, inversions, rearrangements, gain or loss of whole or large portions of chromosomes, and translocations [1]. An earlier study identified somatic mutations in five genes including *MRE11*, *ZW10*, *ZWILCH*, *ROD*, and *DING*, among 100 human CIN-candidate genes that shared similarity with yeast or fly "instability" genes [2]. Their data suggested that at least one of three functions including double-strand break repair, kinetochore function, and chromatid segregation, is impaired in CIN tumors by somatic mutation. Another study searched for mutations of 102 human homologues of yeast CIN genes in 132 colorectal cancers. Consequently, they identified a total of 11 mutations in five genes that included four associated with sister chromatid cohesion (*SMC1L1*, *CSPG6*, *NIPBL*, and *STAG3*, the homologues of yeast *SMC1*, *SMC3*, *SCC2*, and *SCC3*, respectively) [3]. Since sister chromatid cohesion is indispensable for cellular processes such as chromosome segregation, homologous recombinational repair, and regulation of transcription [4], genetic alterations in the components and regulators should play a crucial role in the CIN of colorectal tumors.

We previously performed gene expression profile analysis in CRC [5], and identified that DNA replication and sister chromatid cohesion 1 (*DSCC1*, also known as *DCC1*) was frequently elevated in colorectal tumors compared with non-cancerous colonic mucosa. Dcc1p, a homolog of DSCC1, was first identified as a member of alterative replication factor C (RFC) complex in the yeast, and physically associates with Ctf8p and Ctf18p [4]. Deletion of the component, Ctf18p, Ctf8p, or Dcc1p, resulted in severe sister chromatid cohesion defects, and increased sensitivity to microtubule depolymerizing drugs, suggesting that these components are essential for maintenance of chromatin integrity [4]. Although Dcc1p was not essential for the viability of yeast, deletion of Dcc1p led to synthetic lethality in combination

with mutation of other sister chromatid cohesion proteins [6]. In addition to the implication in sister chromatid cohesion, the CTF18-DSCC1-CTF8-RFC complex plays a crucial role in DNA replication through the interaction with single-stranded and primed DNA as a loader of proliferating cell nuclear antigen [7]. Furthermore, genetic network analysis of functionally related genes in the yeast suggested that the components of CTF18-DSCC1-CTF8-RFC complex interact with the MAD/BUB spindle checkpoint pathway, the RAD51 DNA repair pathway for double-strand breaks, the RAD9 DNA damage checkpoint, and the TOF1/MRC DNA replication checkpoint pathway [8,9]. The finding that mutation in CTF18-RFC increased triplet repeat instability corroborated the role of this complex in the DNA-replication checkpoint [10]. These data indicated that DSCC1 plays an important role in replication, spindle checkpoint and DNA repair, which prompted us to investigate whether deregulated expression of DSCC1 is involved in human colorectal tumorigenesis.

Here, we show for the first time that DSCC1 is frequently up-regulated in CRC at least in part through the enhanced transcriptional activation by E2F. We also reveal that elevated expression of DSCC1 confers chemoresistance in CRC cells by providing tumor cells with anti-apoptotic properties. These findings will contribute to a better understanding of CRC, and serve as a starting point for the development of novel strategies for diagnosis and treatment of CRC.

Materials and Methods

Ethics statement

This project was approved by the ethical committee of Institute of Medical Science, the University of Tokyo (IMSUT-IRB, 21-14-0806). Written informed consent was obtained from all patients in this study. All colorectal cancer tissues and corresponding non-cancerous tissues were obtained from surgical specimens of patients who underwent surgery.

Cell culture

Human CRC cell lines HCT116, HCT-15, SW480, DLD-1, LoVo, Caco-2, LS174T, HT-29, and RKO were purchased from the American Type Culture Collection (Manassas, VA). All cells were grown in appropriate media supplemented with FBS (Life Technologies, Carlsbad, CA) and antibiotic/antimycotic solution (Sigma, St. Louis, MO).

Preparation of plasmids expressing DSCC1 and E2Fs

The entire coding region of *DSCC1* cDNA (GenBank accession No. NM_024094) was amplified by RT-PCR using a set of primers; forward primer: 5′-CCGGAATTCATGAAGAG-GACCCGCGAC-3′ and reverse primer: 5′-CGGCTCGAGA-GAAATGGGTCTTCTCGAATTAT-3′ (underlined nucleotides indicate the recognition sites of restriction enzymes). The PCR products were cloned into the *Eco*RI and *Xho*I sites of pcDNA3.1/myc-His. We additionally generated plasmids expressing HA-tagged DSCC1 (pCAGGS-DSCC1). The constructs pcDNA3-HA-E2Fs were kindly provided by Dr. J. R. Nevins (Duke University, Durham, NC).

Quantitative PCR and gene copy number analysis

Real-time PCR was performed using the LightCycler 480 system (Roche Diagnostics, Indianapolis, IN). Genomic DNAs were extracted from CRC cell lines for copy number analysis. Quantitative PCR was performed on ABI PRISM 7900HT Sequence Detection System, using FAM-labeled probes (5′-TCAGGTTTCCTACCTTCCGGCTGCTT-3′) and a set of primers (forward: 5′-GGCGCGCTTTCAAACG-3′, reverse: 5′-GCGGGCAAGAAAGAAGTTCC-3′) for *DSCC1*, and TaqMan Copy Number Reference Assays RNase P as a quantitative control (Life Technologies). The copy number of *DSCC1* in the cancer cells was calculated in comparison with genomic DNA from healthy volunteers using CopyCaller Software.

Subcellular fractionation and immunoblotting

Cells were lysed in radioimmunoprecipitation assay buffer (50 mM Tris-HCl, pH 8.0, 150 mM NaCl, 0.5% sodium deoxycholate, 1% Nonidet P-40, 0.1% SDS) supplemented with a Protease Inhibitor Cocktail Set III (Calbiochem, San Diego, CA). Nuclear extracts were prepared using Nuclear Extract Kit (Active Motif, Carlsbad, CA). Proteins were separated by SDS-PAGE and immunoblot analysis was performed using the indicated antibodies. Horseradish peroxidase-conjugated goat anti-mouse or anti-rabbit IgG (GE Healthcare, Buckinghamshire, UK) served as the secondary antibody for the ECL Detection System (GE Healthcare).

Immunostaining

Primary antibodies used for immunohistochemical and immunocytochemical staining were anti-DSCC1 (B01P, Abnova, Taipei, Taiwan) and anti-Myc (Sigma). The specificity of DSCC1 antibody was confirmed by the blocking with DSCC1 recombinant protein (data not shown). These experiments were performed as described previously [11].

Induction of apoptosis and flow cytometry

To study the induction of apoptosis, cells were treated with camptothecin (Wako, Osaka, Japan), doxorubicin (LC Laboratories, Woburn, MA), MG132 (Merck Millipore, Darmstadt, Germany), or exposed to γ-irradiation (Gammacell 40, Atomic Energy of Canada, Ontario, Canada). Expression of cleaved poly (ADP-ribose) polymerase (PARP) and cleaved caspase-3 was detected by western blot analysis using anti-cleaved PARP (9541) and anti-caspase-3 antibodies (9662), respectively (Cell Signaling Technology, Danvers, MA). Assessment of apoptosis was also performed by annexin V and PI double-staining using Alexa Fluor 488 Annexin V/Dead Cell Apoptosis Kit (Life Technologies). Briefly, cultured cells were treated with vehicle or camptothecin for 24 h. The cells were stained with Annexin V and PI, and subsequently analyzed on a FACSCalibur (Becton Dickinson, Franklin Lakes, NJ) using FlowJo software (Tree Star, Ashland, OR).

Cell viability assay

Plasmids expressing short hairpin RNA (shRNA) using U6 promoter (psiU6BX3.0) were prepared as described previously [12]. Plasmids expressing DSCC1 shRNA (psiU6-shDSCC1) were constructed by cloning double-stranded oligonucleotides into the *Bbs*I sites of the psiU6BX3.0 vector. Two target sequences, 5′-GUGGACAGAAGAAGAUAUU-3′ (shDSCC1#1) and 5′-GCAAACCAUAGGUGCAUUA-3′ (shDSCC1#2), were used for DSCC1 shRNAs. As negative controls, we prepared a plasmid targeting enhanced green fluorescent protein (psiU6-shEGFP) and those targeting scrambled sequences of shDSCC1#1 (5′-AAAUUGCGAAGGUGAUGAA-3′; psiU6-shDSCC1#1scr) or shDSCC1#2 (5′-AACACGUUAAUAACCGGUG-3′; psiU6-shDSCC1#2scr). Cell viability assays were carried out as described previously using HCT116, SW480, and RKO cells transfected with plasmids expressing shEGFP, shDSCC1, or

scramble shDSCC1 [11]. To investigate the effect of DSCC1 overexpression on cell proliferation, we transfected SW480 and HCT116 cells with pCAGGS-DSCC1 and established two or three clones stably expressing exogenous DSCC1. Control SW480 and HCT116 cells transfected with empty vector were also established as mock cells.

Promoter reporter assays and site-directed mutagenesis

Luciferase reporter plasmids containing the *DSCC1* promoter were prepared by cloning the 5′-flanking region of *DSCC1* into the *Mlu*I and *Bgl*II restriction enzyme sites of pGL3-Basic vector (Promega, Madison, WI). A DNA fragment of approximately 1.0-kb in the 5′-flanking region of *DSCC1* was amplified by PCR using genomic DNA from healthy volunteers and a set of primers (forward: 5′-CGACGCGTATGTCTGCTCAGATCCTTT-GAAT-3′, reverse: 5′-GAAGATCTCGCCGGGTCTAG-GAGTCC-3′). Mutant plasmids containing substitutions in putative E2F binding sites of the *DSCC1* promoter were generated by site-directed mutagenesis using the QuikChange II XL Site-Directed Mutagenesis Kit (Agilent Technologies, Santa Clara, CA). Cells seeded into 6-well plates were transfected with the reporter plasmids together with pRL-TK (Promega) using FuGENE 6 reagent. Cells were harvested 24 hours after transfection, and reporter activities were measured by dual luciferase system (TOYO B-Net, Tokyo, Japan). For the knock-down of E2F1 expression, synthetic E2F1 siRNA was purchased from Sigma (sense: 5′-GGGAGAAGUCACGCUAUGA-3′, anti-sense: 5′-AUAGCGUGACUUCUCCCCC-3′).

Chromatin immunoprecipitation assay

To investigate the interaction of E2F1 with the *DSCC1* promoter region, a chromatin immunoprecipitation (ChIP) assay was performed according to the Agilent Mammalian ChIP protocol with slight modifications. HCT116 cells were cross-linked with 1% formaldehyde for 10 min at room temperature and quenched with 0.4 M glycine. Chromatin extracts were sheared by micrococcal nuclease digestion, and subsequently protein-DNA complexes were immunoprecipitated with 3 μg of anti-E2F1 polyclonal antibody (C-20, Santa Cruz Biotechnology, Santa Cruz, CA) bound to anti-rabbit IgG-coated Dynabeads (Life Technologies). Non-immune rabbit IgG (Santa Cruz Biotechnology) was used as a negative control. The precipitated DNAs were subjected to quantitative PCR analysis with a primer set (forward (−26) 5′-CCGGAAACACGCCCATGGC-3′ and reverse (+127) 5′-GGGTCCTCTTCATCGCAGC-3′) to amplify the *DSCC1* promoter region. Specificity of the assay was determined by the amplification of a distal upstream region in the *DSCC1* promoter with the following primers: forward (−1279) 5′-AGTTGTAGG-GAATGTTTCCCATT-3′ and reverse (−1111) 5′-GATTGGTTCATGTGACCTACTTC-3′. In addition, the amplifications of cell division cycle 2 (*CDC2*) promoter and glyceraldehyde-3-phosphate dehydrogenase (*GAPDH*) promoter were used for positive and negative controls, respectively (primers: *CDC2* forward 5′-CGCCCTTTCCTCTTTCTTTC-3′, *CDC2* reverse 5′-ATCGGGTAGCCCGTAGACTT-3′, *GAPDH* forward 5′-TACTAGCGGTTTTACGGGCG-3′, *GAPDH* reverse 5′-TCGAACAGGAGGAGCAGAGAGCGA-3′).

Results

Expression of DSCC1 is frequently elevated in CRC

In order to identify novel target molecules for the treatment and/or diagnostic biomarkers of CRC, we previously performed expression profile analysis of colorectal tumors and their matched normal colorectal tissues by cDNA microarray [5]. Among the genes deregulated in colorectal tumors, expression of DNA replication and sister chromatid cohesion 1 (*DSCC1*) was increased more than two-fold in 5 of 7 colorectal cancers compared with corresponding non-cancerous colon mucosa (Figure 1A). Subsequent real-time PCR analysis using an additional 20 CRC tissues and the corresponding non-cancerous mucosa revealed that *DSCC1* expression was elevated more than two-fold in 12 of the 20 tumors (Figure 1A). An immunohistochemical staining showed accumulated DSCC1 protein in 29 of 40 CRC tissues compared with corresponding adjacent non-cancerous colonic mucosa (Figure 1B). Although we searched for correlations between its expression and clinicopathological factors including age and sex of the patients, location, size, and histological data of the tumors such as depth of invasion, lymph node involvement, and vascular or lymphatic vessel invasion, none of the factors was significantly associated with DSCC1 expression (Table S1). Additionally, western blot analysis using CRC cell lines revealed that DSCC1 was abundantly expressed in HCT116, HT-29, and DLD-1 cells, and that it was expressed at low levels in SW480, SW620, and Caco-2 cells (Figure 1C). Although we compared stability of DSCC1 protein in HCT116 (DSCC1-high) and SW480 (DSCC1-low) cells by cycloheximide chase assay, DSCC1 was relatively stable in both HCT116 and SW480 cells. Treatment with MG132, a proteasome inhibitor also did not enhance DSCC1 expression (Figure S1A). These data suggested that protein stability is not likely to play a major role in the elevated expression of DSCC1 in cancer cells.

Immunohistochemical analysis unexpectedly depicted accumulated DSCC1 in the cytoplasm and nucleus of DSCC1-positive cancer cells (Figure 1B), although Dscc1 was reported to play a role in the establishment of cohesion during DNA replication in the yeast. To elucidate its subcellular localization, we carried out immunocytochemical staining of endogenous DSCC1 in HCT116 cells. Consistent with the immunohistochemical staining of cancer tissues, DSCC1 protein was localized in both cytoplasm and nucleus (Figure 1D and S1B). Furthermore, western blot analysis using cytoplasmic and nuclear fractions extracted from HCT116, RKO, and DLD-1 cells (Figure 1E) and cells expressing Myc-tagged DSCC1 confirmed its subcellular localization in the cytoplasm as well as the nucleus (Figure S1C and S1D).

Copy number analysis of *DSCC1*

To address whether gene amplification is involved in the DSCC1 overexpression, we conducted copy number analysis by quantitative PCR using RNase P as a control. Compared with peripheral leukocytes from healthy volunteers, the copy number of *DSCC1* was not increased in any CRC cell lines tested (Figure 1F). It is worth noting that a decrease in copy number was observed in HT-29 cells that abundantly expressed DSCC1 (Figure 1C). We further analyzed copy number alteration of *DSCC1* in colon and rectum adenocarcinoma (The Cancer Genome Atlas Colorectal Cancer project) using the cBioPortal database (http://www.cbioportal.org/public-portal/). As a result, putative copy number changes were found in 7 of 257 colorectal adenocarcinomas (2.7%), suggesting that amplification of *DSCC1* does not play a major role in the enhanced DSCC1 expression.

Regulation of *DSCC1* promoter activity

To resolve the mechanism of elevated DSCC1 expression in CRC, we investigated the promoter activity of *DSCC1* in HCT116 cells. Reporter assay using plasmids containing a 5′-flanking region of *DSCC1* (pDSCC1-1023/+109) showed that this region has a substantial promoter activity (data not shown). In the region,

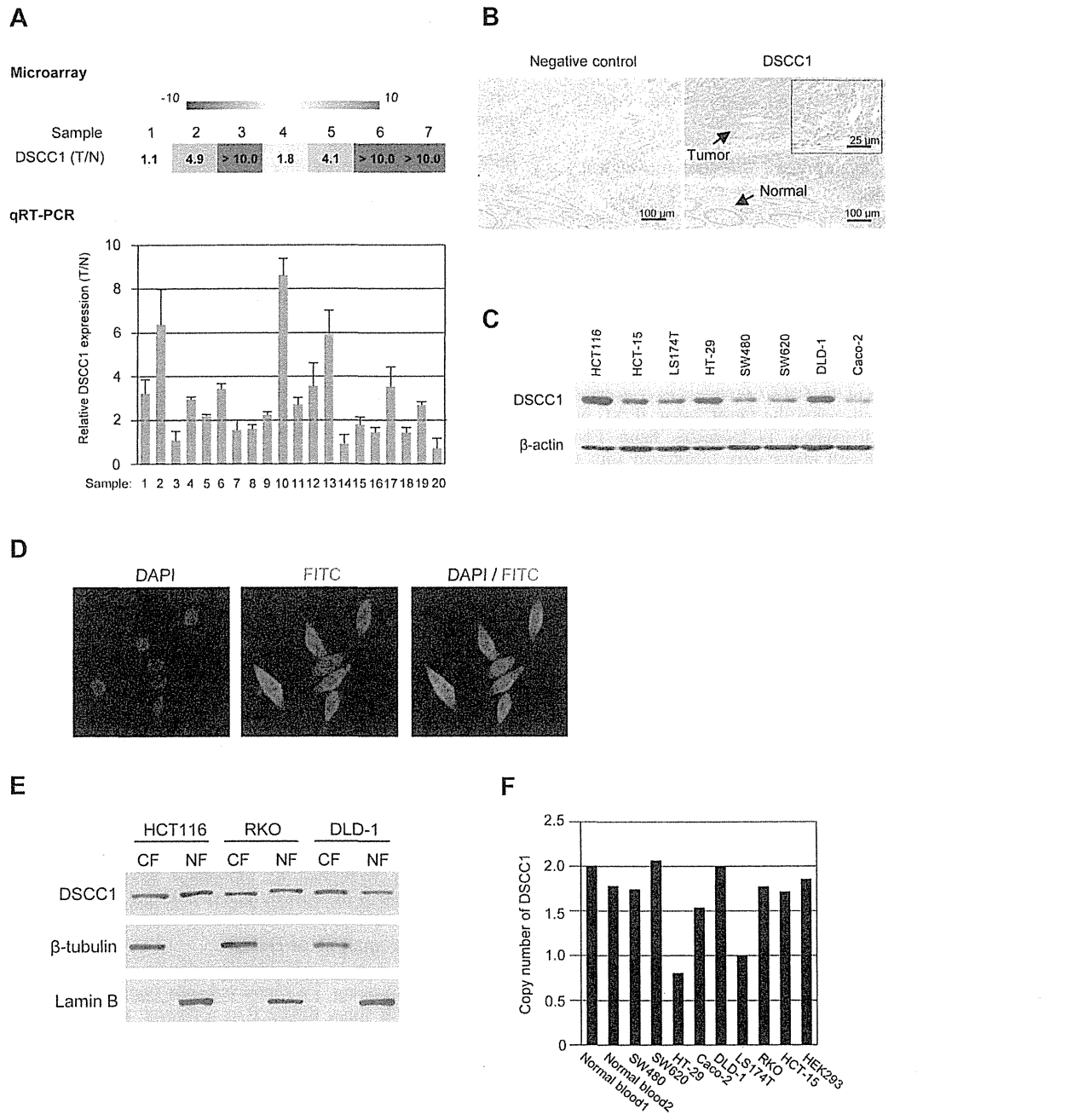

Figure 1. Expression of DSCC1 in colorectal tumors. (A) Relative expression ratios of *DSCC1* in seven colorectal cancer tissues to their corresponding normal tissues in our microarray data (upper panel). Relative expression levels of *DSCC1* in an additional 20 colorectal tumors and the corresponding non-cancerous mucosa was analyzed by quantitative PCR (lower panel). Quantity of *DSCC1* was normalized to *HPRT1* expression. Y axis indicates the ratio of mean of *DSCC1* expression in tumor to that in their corresponding normal tissue. The data represents mean ± SD from triplicate experiments. (B) Representative image of immunohistochemical staining of DSCC1 in a human colon cancer tissue containing cancer cells and adjacent normal mucosa. (C) Expression of DSCC1 in CRC cell lines was detected by western blotting using anti-DSCC1 antibody. (D) HCT116 cells were probed with anti-DSCC1 antibody followed by FITC-conjugated anti-mouse IgG secondary antibody (green). Nuclei were counter-stained with DAPI (blue). (E) HCT116, RKO, and DLD-1 cells were separated into the cytoplasmic (CF) and nuclear fractions (NF), and the cytoplasmic and nuclear proteins were subjected to SDS-PAGE followed by western blotting. Purity of the fractions was determined by the presence of β-tubulin (cytoplasmic marker) and lamin B (nuclear marker). (F) Copy number analysis of *DSCC1* in eight CRC cell lines and HEK293 cells. Relative copy number of *DSCC1* gene was determined by quantitative PCR using *RPPH1* as an endogenous reference. The copy number was calculated by dividing their PCR products by those of peripheral leukocytes from healthy volunteers, and subsequently multiplying by 2.
doi:10.1371/journal.pone.0085750.g001

we identified a putative E2F-binding motif, EBS1 (−3/+5; 5′-CTTGGCGC-3′) using the JASPAR (http://jaspar.genereg.net/) and TFSEARCH databases (http://www.cbrc.jp/research/db/TFSEARCH.html) (Figure 2A). This putative binding site shared high similarity with the consensus motif for E2F, TTTSSCGC with S = G or C. Since E2F transcription factors are frequently deregulated in a variety of tumors, we tested the effect of E2Fs on the *DSCC1* promoter activity. Although E2F1, E2F2, E2F3, and E2F4 increased the promoter activity, E2F6 did not change the activity. E2F1, which showed the strongest induction among the four members, augmented the activity in a dose-dependent fashion (Figure 2B and S2A). This enhancement was also observed in other cell lines including LoVo, HeLa, and HEK293 (data not shown). To examine the possible involvement of EBS1 in the enhancement, we measured reporter activity using the constructs pDSCC1-10/+109 and +10/+109 in the presence or absence of E2F1 (Figure 2C). Basal reporter activities of these reporter plasmids were not significantly different in the absence of E2F1 plasmids. Deletion of EBS1 (pDSCC1+10/+109) dramatically decreased E2F1-induced reporter activity (from 20.4-fold to 3.2-fold). Unexpectedly, enhancement of reporter activity by E2F1 was still observed in +10/+109. Further deletion up to +70 of the promoter (pDSCC1+70/+109) completely diminished E2F1-induced reporter activity (Figure 2C). In agreement with this result, we found two additional presumptive EBSs, EBS2 (+31/+38; 5′-CTTCCGGC-3′) and EBS3 (+57/+64; 5′-TTGCCCGC-3′) in the region between +10 and +70. To address responsibilities of EBS1, EBS2, and EBS3 for the induction, we prepared four mutant reporter constructs (Figure 2D) by substituting the GC-rich segment in E2F consensus motifs, TTTSSCGC (S = C or G) or STTTS, because these core motifs were reportedly crucial for E2F binding [13,14]. Compared with wild type pDSCC1-10/+109 (14.8-fold induction), both types of EBS1-mutant plasmids (pDSCC1-10/+109 mut1, and mut1′) remarkably decreased the reporter activity in response to E2F1 (5.2-fold and 5.8-fold, respectively). Mutations in both EBS1 and EBS2 (pDSCC1-10/+109 mut1+2) further decreased in the E2F1-induced activity (3.7-fold). Mutant reporter plasmid containing substitutions in the three elements (pDSCC1-10/+109 mut1+2+3) almost diminished the enhancement (1.7-fold), suggesting that the three E2F binding motifs are responsible for the regulation of *DSCC1* promoter activity.

Interaction of E2F1 with the *DSCC1* promoter region

To determine whether E2F1 binds to the promoter region of *DSCC1*, we performed quantitative ChIP assay using anti-E2F1 antibody and a set of primers encompassing the three putative E2F-binding elements. The promoter of cell division cycle 2 gene (*CDC2*), a well-known E2F1 target, was enriched 13.4-fold with the immunoprecipitated DNA (Figure S2B). Expectedly, the *DSCC1* promoter region was enriched by up to 15.4-fold in the DNA, suggesting an interaction of the *DSCC1* promoter region with E2F1 (Figure 2E).

To confirm the involvement of E2F1 in regulating DSCC1 expression, we investigated the silencing effect of E2F1 on DSCC1 expression. Real-time PCR and western blot analyses showed that depletion of E2F1 decreased DSCC1 expression (Figure 2F and S2C). RNAi-mediated knockdown of E2F1 activity was confirmed by reporter assay showing significant reduction of the *DSCC1* promoter activity from 10.4 (Ctrl siRNA) to 4.7-fold by E2F1 siRNA in SW480 cells (Figure 2G). These results suggested that *DSCC1* transactivation is, at least in part, regulated by E2F1 in CRC through its interaction with the *DSCC1* promoter region, and that the three EBSs play an important role in the transcriptional activation. To further investigate whether DSCC1 expression is modulated by E2F transcriptional activity, we compared the relative expression of *DSCC1* with *CDK1* (*CDC2*), as readout of E2F transcriptional activity, using two independent data sets (E-MEXP-3715 and GEOD-23878) in the Gene Expression Atlas database (http://www.ebi.ac.uk/gxa/). In the data sets, *DSCC1* and *CDK1* were significantly up-regulated in colorectal tumors compared with normal colonic tissues (Figure 3). Notably, both data sets calculated high values of correlation coefficient (E-MEXP-3715, $r = 0.912$ and GEOD-23878, $r = 0.864$) between *DSCC1* and *CDK1*, supporting the view that *DSCC1* is another downstream gene regulated by E2F.

Effect of DSCC1 on the proliferation of CRC cells

To address the role of its elevated expression in CRC cells, we investigated whether DSCC1 is involved in the proliferation of cancer cells. We carried out cell viability assay using plasmids expressing both DSCC1 shRNA (shDSCC1#1, or shDSCC1#2) and neomycin resistant gene. Plasmids containing the scrambled sequence of DSCC1 shRNAs (shDSCC1#1scr and shDSCC1#2scr) and plasmid containing EGFP shRNA (shEGFP) served as controls. Transfection with these DSCC1 shRNAs (shDSCC1#1, or shDSCC1#2) reduced the expression of DSCC1, whereas transfection with controls (shEGFP, shDSCC1#1scr and shDSCC1#2scr) had no effect (Figure 4A). HCT116 cells were cultured in media containing appropriate concentration of G418 and the cell viability was measured. We found that the number of viable cells transfected with DSCC1#1 or DSCC1#2 shRNA was significantly decreased compared to those transfected with EGFP, DSCC1#1scr, or DSCC1#2scr shRNA, indicating that DSCC1 plays a role in the viability of cancer cells (Figure 4B). Consistent data was obtained in SW480 and RKO cells (Figure S3A). These results were confirmed in repeated experiments.

In addition, we established SW480 cells that constitutively express exogenous DSCC1, and compared their proliferation with control cells transfected with mock vector (Figure 4C). Consistent with the DSCC1-knockdown data, cells expressing exogenous DSCC1 showed augmented cell proliferation compared to parental SW480 cells or control cells ($p = 2.2 \times 10^{-5}$). Similarly, exogenous DSCC1-expression enhanced the proliferation of HCT116 cells (Figure S3B).

Role of DSCC1 in the induction of apoptosis

Since E2F1 conferred resistance to genotoxic insults [15,16,17], we further investigated whether elevated DSCC1 expression plays a role in the sensitivity of cancer cells to genotoxic stimuli. SW480 cells-expressing exogenous DSCC1 (SW480-DSCC1#1, #3, and #8) were exposed to γ-irradiation, and induction of apoptosis was analyzed by immunoblotting with anti-cleaved PARP antibody. As shown in Figure 5A, quantification of cleaved PARP-specific bands revealed that γ-irradiation led to 3.9, 2.6, and 1.2-fold increase of cleaved PARP in control cells (SW480-Mock#1, #3, and #4, respectively). On the other hand, 1.0, 1.4, and 1.2-fold increase was observed in response to γ-irradiation in SW480-DSCC1#1, #3, and #8 cells, respectively, suggesting that DSCC1 suppressed apoptosis by γ-irradiation. In addition, treatment with camptothecin, an inhibitor of topoisomerase I, induced early apoptotic cells (annexin V-positive and PI-low) by 5.6±2.9% in control cells (Figure 5B), while the treatment increased early apoptotic cells by only 0.7±0.3% in SW480-DSCC1 cells, indicating a significant suppression of apoptosis ($p = 0.02$). These data suggested that elevated DSCC1 expression might confer resistance to apoptotic stimuli in cancer cells. In

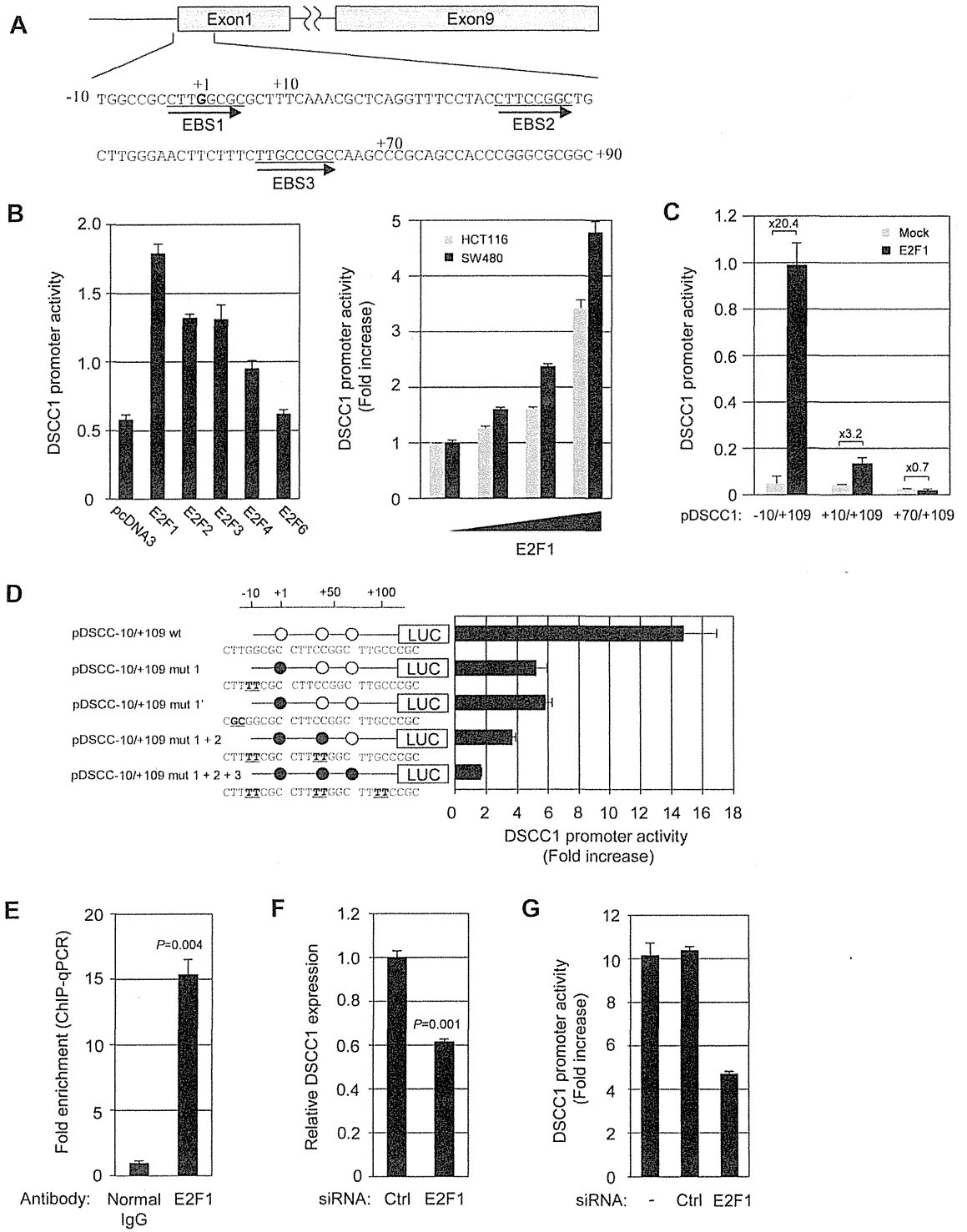

Figure 2. Regulation of *DSCC1* promoter activity by E2F transcription factor. (A) Nucleotide sequence of the −10 to +90 bp region human *DSCC1*. Three putative E2F binding motifs are underlined. (B) pDSCC1-1023/+109 was transiently transfected with pRL-TK and pcDNA3 HA-E2Fs into SW480, or with pRL-TK and pcDNA3 HA-E2F1 (0.01-1 μg) into SW480 and HCT116 cells. (C) pDSCC1-10/+109 or the shorter promoter constructs was transfected with E2F1 or the empty vector into SW480 cells. (D) Site-directed mutation analysis of putative E2F binding sites in the proximal promoter region. pDSCC1-10/+109 or its mutant clones was transfected with E2F1 or the empty vector into SW480 cells. The data represents mean ± SD from three independent experiments. Promoter activity indicates the relative luciferase unit or the fold induction over empty vector transfectant. (E) Chromatin immunoprecipitation was performed using anti-E2F1 antibody. The precipitated DNAs were subjected to the amplification of *DSCC1*

promoter by quantitative PCR. To ascertain the specific binding to the EBS, the amplification of a distal upstream region in the *DSCC1* promoter was used for normalization. A significant difference was determined by t-test. (F) HCT116 cells were transfected with control or E2F1 siRNA (25 nM) for 48 h. *DSCC1* expression was detected by quantitative PCR. A significant difference was determined by t-test. (G) SW480 cells were transfected with control or E2F1 siRNA (25 nM), followed 8 h later by transfection with reporter plasmid (pDSCC1-10/+109) and E2F1 expression vector or the empty vector. After 48 h, luciferase activity was measured. The data represents mean ± SD from three independent experiments.
doi:10.1371/journal.pone.0085750.g002

complete agreement with these results, knockdown of DSCC1 potentiated camptothecin- and γ-irradiation-induced apoptosis in HCT116 cells (Figure 5C and S3C). To address whether DSCC1 expression affects cell death induced by other types of cytotoxic reagents, we treated HCT116 cells with doxorubicin, a DNA intercalator, or MG132, a proteasome inhibitor, and measured the cleavage of PARP and caspase-3, indicators of apoptosis. Suppression of DSCC1 augmented the cleavage of PARP and caspase-3 in response to doxorubicin, whereas knockdown of DSCC1 did not increase the cleavage in response to MG132 (Figure S3D and S3E). Therefore, DSCC1 may be associated with the cell death caused by DNA-damage, but not with the death by other types of cytotoxic insults. Of note, DSCC1 depletion also enhanced induction of apoptosis by γ-irradiation in p53-null HCT116 cells (Figure S3F), suggesting that DSCC1-mediated resistance against apoptosis was independent of p53. These results imply that suppression of DSCC1 may be useful for the treatment and/or chemosensitization of CRC cells.

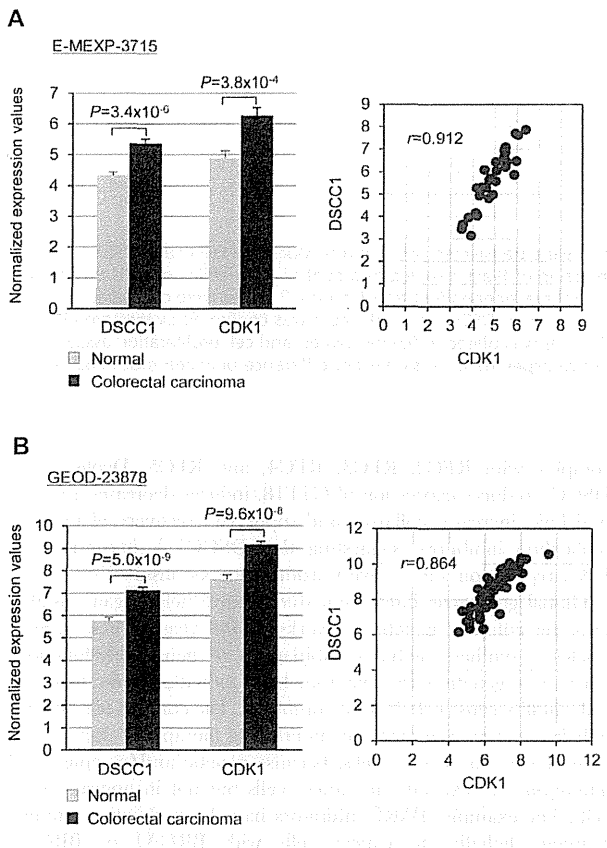

Figure 3. Positive correlation between *DSCC1* and *CDK1* expression in colorectal tumors. This association was shown by two sets of microarray data, E-MEXP-3715 (A) and GEOD-23878 (B), in the Gene Expression Atlas database (http://www.ebi.ac.uk/gxa/). The Pearson's correlation coefficient (r) between *DSCC1* and *CDK1* expression values was then calculated to assess their correlation.
doi:10.1371/journal.pone.0085750.g003

Discussion

Regulated by the retinoblastoma tumor suppressor, pRB, and/or related proteins, E2Fs play crucial roles in cell cycle, nucleotide synthesis, DNA replication, DNA repair, and apoptosis [18,19]. Activities of E2Fs are regulated by integration of signals transduced from the cellular DNA and the external environment. E2F1 is thought to act as an oncogene and a tumor suppressor, with its action dependent on the cellular context. Indeed, overexpression of E2F1 is observed in CRC cells, suggesting its tumorigenic role in the cancer [20]. E2F1 expression is elevated in lung metastasis of colon cancer, and correlates with thymidylate synthase expression, resulting in chemoresistance [21]. On the other hand, E2F1 is over-expressed in colon tumors with increased apoptosis and low proliferation [22]. Therefore, clarification of E2F1 targets should give a clue how this versatile transcription factor family is involved in colorectal carcinogenesis. We have demonstrated here that DSCC1 is frequently up-regulated in CRCs through the transactivation by the E2F family of transcription factors. Although *DSCC1* is located at chromosomal region 8q, which is one of the most frequently amplified chromosomal regions in colorectal tumors [23], copy number gain or amplification was not involved in DSCC1 up-regulation. Instead, we showed here that the flanking region of *DSCC1* transcription start site containing three E2F regulatory sites (EBS1, 2, and 3) plays a role in the transcriptional activation. A previous genome-wide ChIP-chip analysis reported that 20,000–30,000 E2F1-biding sites are distributed over the human genome, of which 51% overlapped transcription start sites [24]. The localization of EBS1, 2, and 3 is compatible with their findings. Among the three sites, EBS1 and EBS3 contain identical sequence with the core E2F1-binding motif (C/GC/GCGC), but EBS2 contains a 1-bp mismatch to the motif. Comparison of human and mouse *DSCC1* 5′-flanking sequences determined that EBS1, located at the −3 to +5 bp region, was well-conserved between the two species (Figure S4A). Consistent with these data, the mutation in EBS1 most remarkably reduced the E2F1-induced promoter activity among the three. Regarding other regulatory elements, we identified a region between −40 and −20 that was associated with basal promoter activity of *DSCC1* (Figure S4B). A search of transcription factor-binding elements in this region found a GC box encompassing a putative ELK1-binding site, but our reporter assay did not show significant change of the promoter activity by ELK1 (data not shown), suggesting that ELK1 may not be involved in the regulation of DSCC1.

Eight members of the mammalian E2F family have been recognized and characterized. Among these members, E2F1, E2F2, and E2F3 are categorized as transcriptional activators, and E2F4, E2F5, E2F6, E2F7, and E2F8 are categorized as repressors [25,26]. In our promoter assay, E2F1, E2F2, E2F3, and E2F4 induced *DSCC1* promoter activity, but E2F6 did not, showing an inconsistent result with E2F4 in the transcription. Molecular studies have uncovered that E2Fs target genes are regulated not only by their binding to DNA element(s) but also by their interacting proteins such as Rb, p107, p130, polycomb group